Staring Beamforming Method for LEO Satellite Based on Angle Increment Prediction

1st Shuxun Li
School of Electronics and Information Engineering
Harbin Institute of Technology
Harbin, China
shuxun_li@163.com

2nd Weixiao Meng
School of Electronics and Information Engineering
Harbin Institute of Technology
Harbin, China
wxmeng@hit.edu.cn

***Abstract*—Supporting IoV is an important application scenario of 5G. For the lack of 5G terrestrial infrastructure, LEO satellite network has become the focus of research. LEO mega-constellations can provide high-speed, secure and full-time global network services for M2M and IoT in 5G network, with its short delay, low path loss and large number of satellites. With the application of mmWave and Massive MIMO, mega-constellation puts forward higher requirements for the accuracy of beam pointing. Frequent beam switching, or channel estimation, will produce greater overhead. According to the angle information for the terminal initiates the access request, and the estimation of the satellite trajectory, the beam direction of the satellite is predicted. By continuously adjusting the beam, the frequency of beam switching is reduced, and the overhead of angle estimation is reduced.**

***Index Terms*—Beyond 5G, Satellite communication, Staring beamforming**

I. INTRODUCTION

At present, 5G (the 5th Generation mobile communication) has been gradually commercialized. However, the function of 5G is still improving. Since the past four generations of mobile communication are mainly working on person-to-person communication, the 5G needs to achieve the goal of person-to-things, things-to-things, and ultimately interconnection of all things. And providing support for IoV is an important application scenario of 5G [1]. Due to political, economic and natural factors, there are still many blind areas of mobile communication around the world. Actually, according to [2], more than 30% of the global population can not access to the mobile communication networks. The reason why it is difficult to access the Internet is that mobile communication relies too much on the terrestrial infrastructure. By contrast, satellite communication system has the characteristics of wide coverage, long communication distance, distance-independent cost, and infrastructure unaffected by disasters. So satellite communication system can provide low-cost communication coverage solutions for areas with weak 5G coverage, and provide high-speed and secure wireless communication network access services for local users. Satellite communication system can also provide network services for M2M (Machine-to-Machine) and IoT (Internet-of-Things) in 5G network.

Because of its characteristics and advantages, satellite communication system has attracted much attention. Many companies have proposed their own LEO (Low Earth Orbit) mega-constellations[3–6]. However, LEO satellites have lower orbital altitude, which means the visible time with terrestrial terminals is limited. Especially with the increase of communication frequency band, the transmission loss also increases. The satellite beam needs more flexible adjustment and more accurate alignment.

For satellite communications, multiple-antenna techniques can provide spatial degree of freedom, which is a key technology in the development of satellite networks [7]. And multiple-antenna beamforming technique can achieve better capacity performance and mitigate interference, which is an important part for satellite to support IoV. In this paper, we propose a staring beamforming method for LEO satellite antenna array. This method predicts the angle change between the satellite and the terminal according to the orbit information of the satellite, and then adjusts the beam direction. It is applicable to both sides of satellite communication, and can cope with beam pointing offset caused by continuous motion and attitude change.

We describe the scenario and model in section II. And the staring beamforming method will be introduced in section III. In section IV, we would give some performance evaluation, to prove the staring beamforming method's superiority. Finally, the conclusion would be drawn in section V.

II. SCENARIO AND MODEL DESCRIPTION

A. Antenna Array Model

The antenna array model is a classical rectangular grid array. Place the array on the plane YOZ, facing the positive direction of the X-axis. The total number of the antenna elements is N. $N = N_y \times N_z$. Assuming that the antenna elements are isotropic antennas and equidistance. And the directivity function of the antenna elements $f_\epsilon(\theta, \phi)$ is equal to 1, so that we can analyze the the directivity function of the antenna array directly.

$$F(\theta, \phi) = F_a(\theta, \phi) f_\epsilon(\theta, \phi) = F_a(\theta, \phi) \quad (1)$$

This work was supported in part by the National Natural Science Foundation of China (Grant No.61871155), and the China's key R&D Program (Grant No.2020YFE0205800).

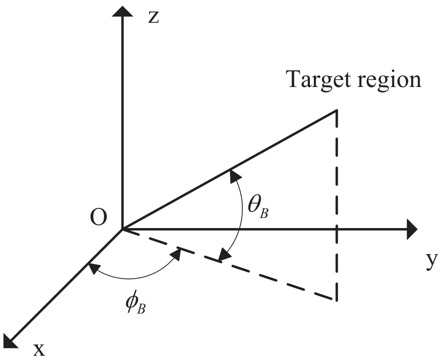

Fig. 1. The relative position of the antenna pointing direction and the array plane.

Affected by the attitude control system, the X-axis of the antenna array is always vertical to the ground and points to the center of the earth. The Y-axis is parallel to the equatorial plane. Use θ and ϕ to describe the pointing direction of the array, as shown in Fig. 1. The directivity function of the antenna array is shown in (2).

$$\begin{aligned} F(\theta,\phi) = \sum_{i=0}^{N-1} a_i \exp\Bigg(j\frac{2\pi}{\lambda}\Big[m_i d_z \sin\theta \\ - m_i d_z \Delta\Phi_\beta + n_i d_y \cos\theta \sin\phi - n_i d_y \Delta\Phi_\alpha \Big]\Bigg) \end{aligned} \tag{2}$$

The a_i is feed coefficient of the i-th element. $(m_i d_z, n_i d_y)$ are used to describe the distance between the element and the center of the antenna array. And the parameter (m_i, n_i) is determined by the position of the element. $\Delta\Phi_\beta$ and $\Delta\Phi_\alpha$ are limited by the pointing direction (θ_B, ϕ_B) of the antenna with (3).

$$\begin{cases} \Delta\Phi_\beta = \sin(\theta_B) \\ \Delta\Phi_\alpha = \sin(\phi_B)\cos(\theta_B) \end{cases} \tag{3}$$

B. Channel Model

The common Ricean channel model is used for satellite communication, and the selection of parameters is based on the suggestions given in the 3GPP technical report 38.811.

For the s-th transmitting antenna and the u-th receiving antenna, the coefficients in the channel matrix are shown in 4. It consists of two parts, namely, line of sight (LOS) path and multipath component.

$$\begin{aligned} H_{u,s}(\tau,t) = \sqrt{\frac{1}{K_R+1}} H_{u,s}^{NLOS}(\tau,t) \\ + \sqrt{\frac{K_R}{K_R+1}} H_{u,s}^{LOS}(\tau,t)\delta(t-\tau_1) \end{aligned} \tag{4}$$

The expression of LOS component is shown in 5. The 4 parts correspond to the phase changes caused by different reasons, which are transmission distance, receiving antenna phase offset, transmitting antenna phase offset, and Doppler frequency shift.

$$\begin{aligned} H_{u,s}^{LOS}(t) = \exp\big(-j2\pi\frac{d_{3D}}{\lambda_0}\big) \exp\big(j2\pi\frac{\hat{r}_{rx,LOS}^T \cdot \bar{d}_{rx,u}}{\lambda_0}\big) \\ \cdot \exp\big(j2\pi\frac{\hat{r}_{tx,LOS}^T \cdot \bar{d}_{tx,s}}{\lambda_0}\big) \exp\big(j2\pi\frac{\hat{r}_{rx,LOS}^T \cdot \bar{v}}{\lambda_0}t\big) \end{aligned} \tag{5}$$

The NLOS component can be written as the sum of multipaths. In the expression of each path, there are 3 factors affecting the phase, which correspond to the receiving antenna phase offset, the transmitting antenna phase offset, and the Doppler frequency shift in turn. The angle information of different paths is generated according to the 3GPP report.

$$\begin{aligned} H_{u,s}^{NLOS}(\tau,t) = \sum_{n=1}^{N} H_{u,s,n}^{NLOS}(t)\delta(\tau-\tau_n) \\ H_{u,s,n}^{NLOS}(t) = \sqrt{\frac{P_n}{M}} \sum_{m=1}^{M} \Big[\exp\big(j2\pi\frac{\hat{r}_{rx,n,m}^T \cdot \bar{d}_{rx,u}}{\lambda_0}\big) \\ \cdot \exp\big(j2\pi\frac{\hat{r}_{tx,n,m}^T \cdot \bar{d}_{tx,s}}{\lambda_0}\big) \exp\big(j2\pi\frac{\hat{r}_{rx,n,m}^T \cdot \bar{v}}{\lambda_0}t\big)\Big] \end{aligned} \tag{6}$$

Satellite communication channel is very sensitive to the angle information of LOS path. Combining the antenna model and the channel model, the process of the satellite passing over the terminal is simulated. The red circle indicates that perfect CSI is used for real-time beamforming, and the blue triangle indicates that LOS angle information is used for beam adjustment. The dotted line corresponding to the color is their regression line. The results show that, whether in low elevation or high elevation scenarios, the performance of beamforming using perfect CSI is slightly higher than relying on the angle information of LOS path. The gain difference is less than 1dB.

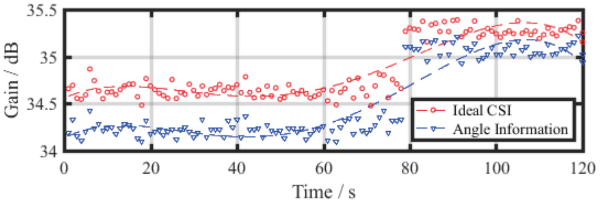

Fig. 2. Array Gain of Low Elevation Scenarios.

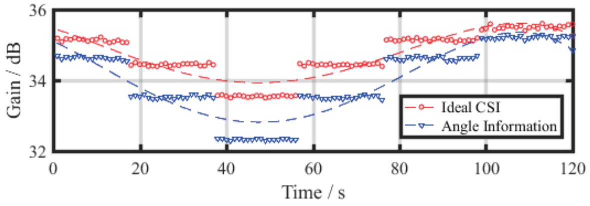

Fig. 3. Array Gain of High Elevation Scenarios.

C. Beamforming Strategy

There are lots of beam-forming algorithms, which can be selected. Each has its own merits. However, in order to adjust beam pointing flexibly, we choose the LCMV algorithm [9]. Since the LCMV algorithm is based on convex optimization, it can give the analytical solution of the weight vector. The LCMV algorithm has superiority on computational complexity and computational speed.

1) Classical LCMV algorithm: The LCMV algorithm aims to ensure that the radiant power of the service area meets requirements. And it would reduce the total transmitting power of the antenna array to the minimum.

Take the receiving antenna as an example. Assuming that the antenna has N elements. For each element, we sampled L times. So we get matrix $\mathbf{X}$, which is a $N \times L$ sampling matrix.

$$\mathbf{X} = \begin{pmatrix} x_1(1) & \dots & x_1(L) \\ \vdots & \ddots & \vdots \\ x_N(1) & \dots & x_N(L) \end{pmatrix} \tag{7}$$

We use $\mathbf{W}$ to represent the weight column vector. And $\mathbf{X}(i)$ is the i-th column vector of the matrix $\mathbf{X}$, which means the simpling of the array at time i. To reduce the antenna output power to minimum, we need to know the expression of the output power. The antenna output at i is (8).

$$y(i) = \mathbf{W}^H\mathbf{X}(i) = \mathbf{X}^H(i)\mathbf{W} \tag{8}$$

And the output power at i is (9).

$$\begin{aligned} \mathbb{E}[y^2(i)] =& \mathbb{E}[\mathbf{W}^H\mathbf{X}(i)\mathbf{X}^H(i)\mathbf{W}] \\ =& \mathbf{W}^H\mathbf{R_{XX}}\mathbf{W} \end{aligned} \tag{9}$$

The $\mathbf{R_{XX}}$ is the autocorrelation matrix of $\mathbf{X}(i)$.

$$\mathbf{R_{XX}} = \mathbb{E}[\mathbf{X}(i)\mathbf{X}^H(i)] \tag{10}$$

If the service area is at (θ_B, ϕ_B), we can get the directivity function of each element at there. We can express it with a column vector $\mathbf{C}$.

$$\mathbf{C} = \begin{pmatrix} \exp[j\frac{2\pi}{\lambda}(m_1 d_z \Delta\Phi_\beta + n_1 d_y \Delta\Phi_\alpha)] \\ \exp[j\frac{2\pi}{\lambda}(m_2 d_z \Delta\Phi_\beta + n_2 d_y \Delta\Phi_\alpha)] \\ \vdots \\ \exp[j\frac{2\pi}{\lambda}(m_N d_z \Delta\Phi_\beta + n_N d_y \Delta\Phi_\alpha)] \end{pmatrix} \tag{11}$$

We hope that with the help of $\mathbf{W}$, the normalized radiated power could be 1. The mathematical expression is (12).

$$\mathbf{W}^H\mathbf{C} = 1 \tag{12}$$

Our purpose is to achieve the minimization of the total output power. The problem of finding the optimum weights $\mathbf{W}$ can be summurized by (9) and (12).

$$\begin{aligned} \text{minimize} \quad & \mathbf{W}^H\mathbf{R_{XX}}\mathbf{W} \\ \text{subject to} \quad & \mathbf{W}^H\mathbf{C} = 1 \end{aligned} \tag{13}$$

The (13) is a convex problem. And the solution of it can be found bu the method of Lagrange multipliers. The derivation process is shown in [8]. The optimal weight vector is (14)

$$\mathbf{W}_{opt} = \mathbf{R}_{\mathbf{XX}}^{-1}\mathbf{C}[\mathbf{C}^H\mathbf{R}_{\mathbf{XX}}^{-1}\mathbf{C}]^{-1} \tag{14}$$

2) Diagonal loading technique: When the number of samples is small, the noise eigenvalue spread is large. It makes the antenna form randomly shaped noise eigenbeams. And the sidelobe level rise. That means the total output power would be wasted. To solve this problem, the [9] developed a kind of improved LCMV algorithm based on diagonal loading technique.

$$\mathbf{R}'_{\mathbf{XX}} = \mathbf{R_{XX}} + \gamma\mathbf{I} \tag{15}$$

$\mathbf{I}$ is the identity matrix. And γ is a real constant representing a small load level. We can use (15) to replace the $\mathbf{R_{XX}}$ in (14). And the solution of the optimal weight vector changes into (16).

$$\mathbf{W}_{opt} = (\mathbf{R_{XX}} + \gamma\mathbf{I})^{-1}\mathbf{C}[\mathbf{C}^H(\mathbf{R_{XX}} + \gamma\mathbf{I})^{-1}\mathbf{C}]^{-1} \tag{16}$$

The noise eigenvalue spread is minimized by the diagonal loading technique. And the random noise eigenbeams is reduced. The performence of the antenna array could be better. Fig. 4 shows the simulation of classical LCMV algorithm. And Fig. 5 shows the simulation of improved LCMV algorithm based on diagonal loading technique. Through the two figures, we can find out that the sidelobe level is reduced by the diagonal loading technique.

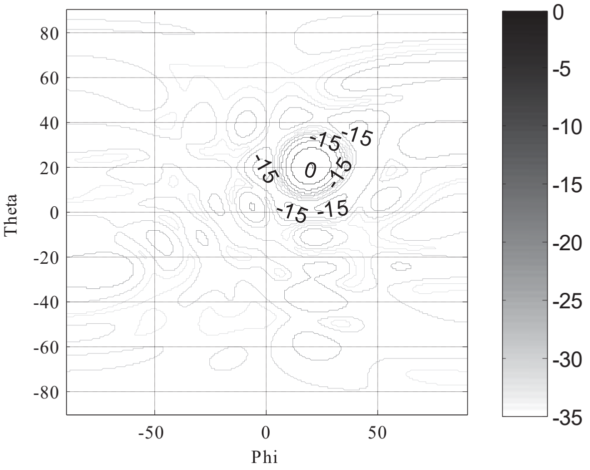

Fig. 4. Simulation of classical LCMV algorithm.

III. STARING BEAMFORMING METHOD

The satellite can obtain the angle information from the terminal through the pilot signal. Therefore, the antenna array can adjust the beam pointing to the terminal according to the angle information. Frequent adjustment means high pilot

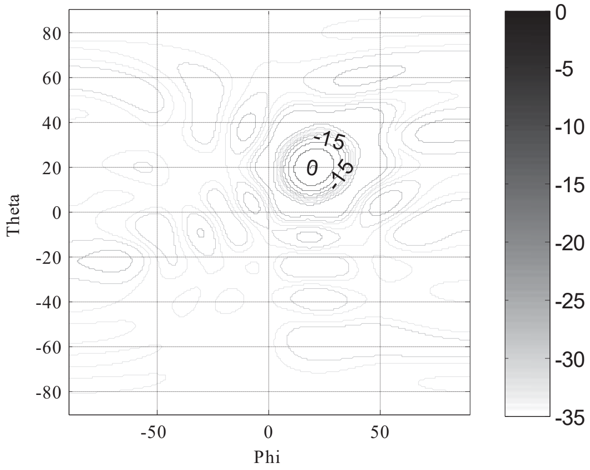

Fig. 5. Simulation of improved LCMV algorithm based on diagonal loading.

signal overhead. At the same time, it is accompanied by a large number of matrix inversion operations. With the increase of scale, the computation of inverse is huge. Staring beamforming needs to reduce angle information estimation and inverse operation.

The on orbit motion of satellites has a very strong law. Therefore, it is easy to obtain the position of satellite. After obtaining angle information, the terminal position can be calculated through coordinate transformation. Then, according to the motion law of the satellite, the change of the beam pointing angle can be calculated.

Assuming the initial value of the pointing angle is (θ_B, ϕ_B). After t seconds, the pointing angle becomes $(\theta_B+\theta_t, \phi_B+\phi_t$. In the directivity function, the phase factor changes.

$$\begin{cases} \Delta\Phi_{\beta,t} \approx \sin(\theta_B) + \cos(\theta_B)\sin(\theta_t) \\ \Delta\Phi_{\alpha,t} \approx \sin(\phi_B)\cos(\theta_B) + \sin(\phi_B)\sin(\theta_B)\sin(\theta_t) \\ +\cos(\phi_B)\cos(\theta_B)\sin(\theta_t) \end{cases} \tag{17}$$

Thus, the angle change (θ_t, ϕ_t) can be obtained through the prediction of the satellite position. Then the weight vector expression is obtained.

$$\mathbf{W}_{staring} = \mathbf{M}_1\mathbf{W}_{opt}\mathbf{M}_2\mathbf{M}_3 \tag{18}$$

where M_1, M_2 and M_3 are diagonal matrix, whose diagonal elements are shown in 19.

$$\begin{cases} m_1(i) = \exp\left(j\frac{2id\pi}{\lambda}\left[\cos(\theta_B)\sin(\theta_t)\right]\right) \\ m_2(i) = \exp\left(j\frac{2id\pi}{\lambda}\left[\sin(\phi_B)\sin(\theta_B)\sin(\theta_t)\right]\right) \\ m_3(i) = \exp\left(j\frac{2id\pi}{\lambda}\left[\cos(\phi_B)\cos(\theta_B)\sin(\theta_t)\right]\right) \end{cases} \tag{19}$$

IV. Performance Evaluation

The staring beamforming method does not need to be iterated, and can quickly obtain the beamforming weight vector. For the simulation of staring beamforming, suppose the terrestrial target is located in Harbin, China. The location of terrestrial target is $127°E, 45°W$. LEO satellite orbit altitude is 800 km. The specific satellite simulation parameters are shown in Table. I.

TABLE I
Orbit parameters of satellite simulation

Parameter	*Value*
Radius of the earth	6371 km
Semi major axis of orbit	7171 km
Orbit eccentricity	0
Orbit inclination	50°
Argument of perigee	70°
Right ascension of ascending node	10°
Perigee passage time	5400 s

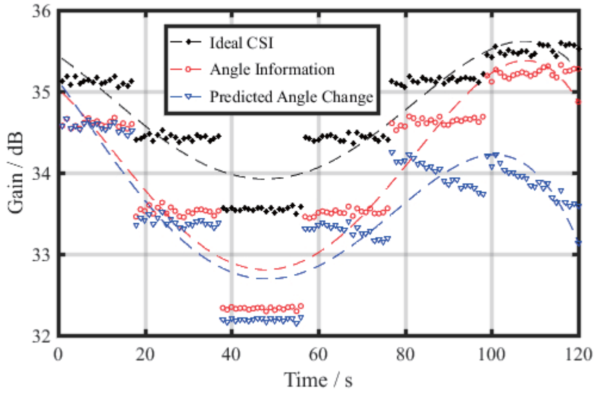

Fig. 6. Gain of Staring Beamforming Algorithm for Satellite Passing Over Target.

The simulation results are shown in Fig. 6. The black asterisk indicates that the perfect CSI is used for real-time beam pointing adjustment, which has the best performance but the largest overhead. The red circle indicates that the angle information is updated in real time and the corresponding pointing adjustment is made. The pointing accuracy is high, but the pilot signal overhead and computation burden are huge. The blue triangle indicates the staring beamforming method. Although the performance is slightly inferior to the best scheme, the angle information is only updated once during the simulation. In terms of overhead, staring beamforming only needs to obtain the initial value of angle information. Moreover, in the process of pointing adjustment, inversion or iteration is not required. This method can flexibly deal with the angular deviation caused by attitude instability. Errors in staring beamforming accumulate. And the closer the terminal is to the center of view, the more sensitive it is to error.

V. Conclusion

The performance of mobile communication system has been greatly improved, and the IoV will become an important scene of 5G application. At the same time, in order to deal with the problem of sparse 5G terrestrial infrastructure, Satellite Internet has become a key solution. Using satellite Internet to provide 5G access service for IoV can not only greatly improve the performance of IoV, but also greatly expand the coverage of 5G network. However, the limitation of satellite visible time requires flexible beam adjustment and accurate beam alignment. On this premise, staring beamforming method can effectively reduce the time of beam switching and prolong the available communication time. Simulation results show that the staring beamforming method can effectively track terrestrial target. Moreover, the staring beamforming method only needs part of CSI for beam alignment, and can cope with pointing mismatch caused by attitude instability. In the service of IoV, compared with directly using a beam to cover all targets, beamforming technology can form multiple spot beams to point to multiple discrete targets, which not only reduces the waste of energy, but also improves the quality of communication, and ensures the coverage of service targets. For the moving vehicles, this method can fulfill the requirements of dynamic multi beamforming. At the same time, staring beamforming method ensures that the beam always points to the visible target covered by the antenna, increases the communication time, and reduces the times of beam switching.

REFERENCES

[1] D. Kombate, Wanglina,“The Internet of Vehicles Based on 5G Communications,” 2016 IEEE International Conference on Internet of Things (iThings) and IEEE Green Computing and Communications (GreenCom) and IEEE Cyber, Physical and Social Computing (CPSCom) and IEEE Smart Data (SmartData), Chengdu, 2016, pp. 445-448.

[2] J. Stryjak, M. Sivakumaran, “The Mobile Economy 2019,” GSMA Intelligence Research Report, February 25, 2019. [Online]. Available: https://www.gsmaintelligence.com/research/2019/02/the-mobile-economy-2019/731/.

[3] “OneWeb Makes History as First Launch Mission is Successful,” OneWeb News, February 28, 2019. [online]. Available: https://www.oneweb.world/newsroom/oneweb-makes-history-as-first-launch-mission-is-a-success.

[4] C. Henry, “SpaceX to launch dozens of Starlink satellites May 15, more Starlink launches to follow,” SpaceNews. May 7, 2019. [Online]. Available: https://spacenews.com/spacex-to-launch-dozens-of-starlink-satellites-may-15-more-starlink-launches-to-follow/.

[5] C. Henry, “Amazon planning 3236-satellite constellation for internet connectivity,” SpaceNews. April 4, 2019. [Online]. Available: https://spacenews.com/amazon-planning-3236-satellite-constellation-for-internet-connectivity/.

[6] M. Wall, “SpaceX Delays Launch of 60 Starlink Internet Satellites Over High Winds,” SpaceNews. May 15, 2019. [Online]. Available: https://www.space.com/spacex-starlink-satellites-launch-delay.html.

[7] X. Zhang, L. Zhu, T. Li, Y. Xia and W. Zhuang, “Multiple-User Transmission in Space Information Networks: Architecture and Key Techniques,” IEEE Wireless Communications, vol. 26, no. 2, pp. 17-23, April 2019.

[8] C. Y. Tseng and L. J. Griffiths, “A simple algorithm to achieve desired patterns for arbitrary arrays” in IEEE Transactions on Signal Processing, vol. 40, no. 11, pp. 2737-2746, Nov. 1992.

[9] C. Y. Cheng, Y. H. Lv. “Application of Improved LCMV Algorithm in Restraining Interference and Noise.” Journal of Electrinic Measurement and Instrument, vol. 20, no. 4, pp. 29-32, 2006.